Measurements of Reynolds stresses in centrifugal compressor vaned diffusers

A Pinarbasi*, **K M Guleren,** and **A Ozturk**
Faculty of Engineering, Department of Mechanical Engineering, Cumhuriyet University, Sivas, Turkey

The manuscript was received on 21 September 2007 and was accepted after revision for publication on 6 March 2008.

DOI: 10.1243/09544062JMES877

Abstract: A phase lock loop sampling technique has been developed in order to perform detailed measurements for the flow field downstream of a turbomachinery rotor. Measurements have been carried out in the vaned diffuser of a low-speed centrifugal compressor using a triple hot wire anemometer. The phase lock loop technique employed in this work has provided a comprehensive representation of the complex three-dimensional unsteady flow in these diffusers. The diffuser vanes were found to have a significant influence on the flow in the vaneless space. The mixing out of the blade wakes is enhanced and accordingly the Reynolds stress levels drop rapidly between the impeller exit and the vane leading edge. The results provide an insight into the flow mechanisms responsible for the losses and hence can be used to develop better design strategies in the future. The flow also exhibits high levels of anisotropy, especially at the mid-vane positions. This suggests that basic Reynolds-averaged Navier–Stokes (RANS) models, including standard one- or two-equation models, might not be sufficient to accurately model the flow in centrifugal compressor diffusers.

Keywords: centrifugal compressor, diffuser flow, Reynolds stress, vaned diffuser

1 INTRODUCTION

In recent years, the performance of most classes of turbomachinery has increased using powerful computers. Also, significant progress has been shown in the field of computational fluid dynamics (CFD) corresponding to the enhancement in the computational power. This progress has positively influenced the modelling of turbomachinery flows. Computers have also been widely used for data acquisition and processing techniques in experimental studies. These are especially important in centrifugal compressor diffusers where the flow is three-dimensional and highly unsteady. One of the major obstacles to improving the reliability in predicting these flows is the uncertainties of classical turbulence models. For the flow, which is dominated by turbulent mixing in a diffuser of the centrifugal compressor, turbulence modelling is undoubtedly very challenging. The entry flow in a diffuser is highly non-uniform and contains significant swirl. This flow is then mixed out as it moves through the diffuser. In the case of a vaned diffuser, the flow is further complicated by the unsteady interaction between the impeller blade wakes and the diffuser vanes. For these reasons, basic turbulence models have not been satisfactorily successful in predicting the complexity of the diffuser flows.

Krain [**1**] investigated the impeller and diffuser flow in a flat straight channel diffuser with a splitter blade impeller. The flow in the vaned diffuser entrance region was highly distorted and unsteady.

Inoue and Cumpsty [**2**] conducted another experimental study using vaneless and vaned diffusers. They observed that the circumferentially averaged mean velocity profile in the axial direction for the vaned diffuser inlet was almost identical with that for the vaneless diffuser. Near the leading edge of the diffuser vane, reversed flow was observed at low flowrates, which led to an increase of loss near the sidewalls.

Davis and Flack [**3**] studied the effect of the number of blades on the performance of a radially vaned diffuser considering three different blade configurations with laser Doppler anemometry (LDA). They measured velocity components for four, six, and eight blades. The turbulence intensities estimated for the

* *Corresponding author: email: alipinarbasi@cumhuriyet.edu.tr*

eight-blade case were the lowest among the considered configurations.

Yoshinaga *et al.* [**4**] used 16 vanes in the diffuser to improve the stage efficiency. Their experimental results are qualitatively in good agreement with potential flow solutions. It was noted that the leading edge orientation has considerable influence on the performance of the diffuser. The features of vaneless diffuser flows in centrifugal compressors have been studied previously by many authors, including Maksoud and Johnson [**5**] and Pinarbasi and Johnson [**6**]. Measurements have been made with LDA, hot wires, and pressure probes. Hot wires have been preferred by many experimentalists because of their low cost and high sensitivity.

Vaned diffusers are applied in a wide variety of compressor applications. Their impact on the operating range of a single-stage compressor depends upon many parameters, including impeller performance, number of vanes, vaneless space ratio, vane thickness, and leading edge configuration. For the diffuser design, the vaneless space ratio is crucially important since it is related to the throat blockage. For example, if the location of the vane leading edge is designed to be very close to the rotor, then the noise level and hence the vibration may increase and high Mach numbers can exist at the vane leading edge.

These studies indicate that flow is highly distorted near the leading edge of the vane, but a well-designed vane diffuser might moderate these non-uniformities. In this study, Reynolds stress measurements for the flow in a vaned diffuser is presented to help the understanding of the flow mixing mechanisms within the diffuser. Moreover, these measurements might be used as reference data for developing advanced turbulence models, which could be used to predict the flow details in the centrifugal compressor with a vaned diffuser configuration.

1.1 Experimental arrangement

The centrifugal compressor, as shown in Fig. 1, has a single stage and is lightly loaded. It has a De Havilland ghost shrouded impeller with 19 backswept blades (Fig. 2). The geometrical parameters and measurement locations of the impeller and diffuser are given in Table 1. As shown in Fig. 3, the vane design has a constant cross-sectional area throughout the vaned diffuser. The absolute Mach number was seen to be around 0.1 in the diffuser.

1.2 Measurement technique

Measurements were made using hot wire anemometry. A triple hot wire probe was used to measure the velocities. A single-wire Dantec (55P11) was aligned circumferentially with a double wire probe Dantec (55P61), wherein each wire of which is slanted 45° in the axial–radial plane as shown in Fig. 4. This mutually perpendicular arrangement of wires was therefore capable of resolving the axial, circumferential, and radial velocity components and the sign of the axial component. The measurements showed that the radial and circumferential velocities were positive. A shaft encoder was used to control simultaneous sampling of output voltages from the hot wire anemometers.

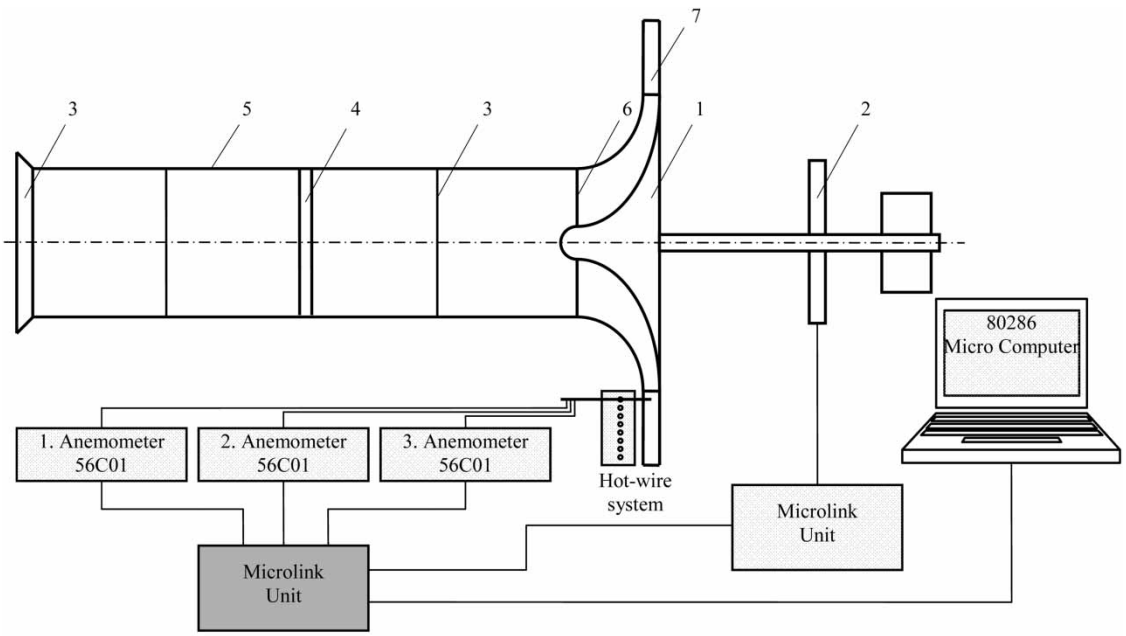


Fig. 1 Schematic of centrifugal compressor test rig

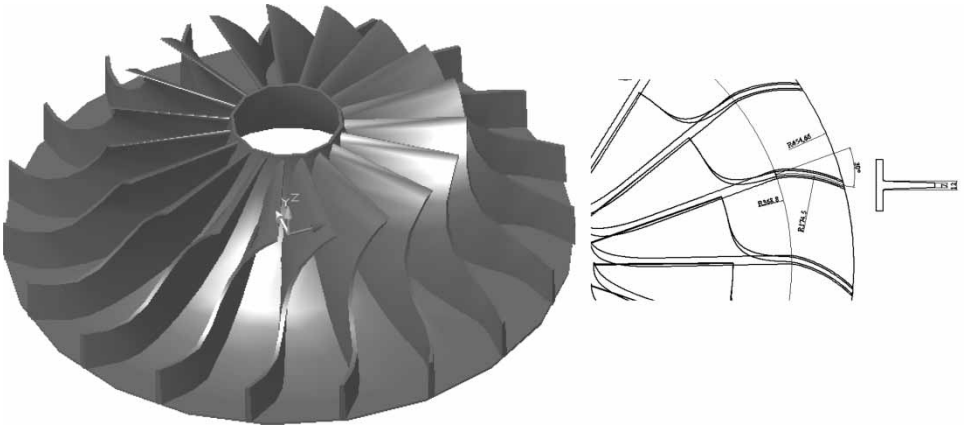


Fig. 2 Backswept impeller blade geometry

Table 1 Geometry, operating conditions, and measurement locations

Impeller	
Inlet blade radius at the hub, R_h	88.75 mm
Inlet blade radius at the shroud, R_s	283.75 mm
Outlet radius, R_o	454.6 mm
Backswept blade angle, β	30°
Number of the blades, N	19
Outlet blade span, b	72.3 mm
Rotating speed, n	500 r/min
Mass flowrate, m	0.1311 kg/s
Vaned diffuser	
Vane geometry	Wedge (included angle 22.5°)
Vane angle	45°
Number of vanes	16
Inlet/outlet area ratio	1
Diffuser throat width	178.5 mm
Diffuser inlet diameter	912.5 mm
Diffuser outlet diameter	1524 mm
Channel length	208.75 mm
Vane span	72.3 mm
Vaneless space radius ratio	1.1
Measurement locations, L/R_o	
Station	
1	0.02
3	0.15

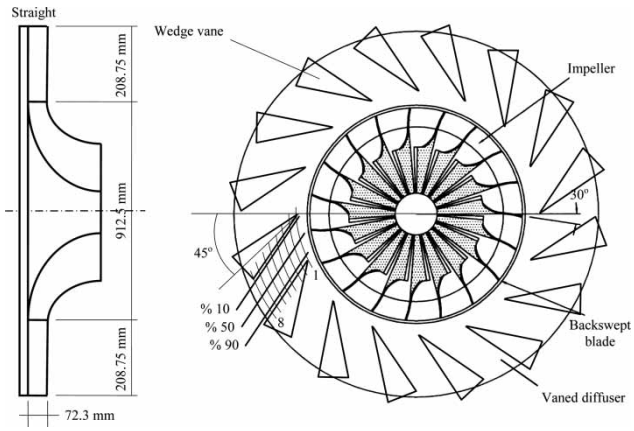


Fig. 3 Diffuser details

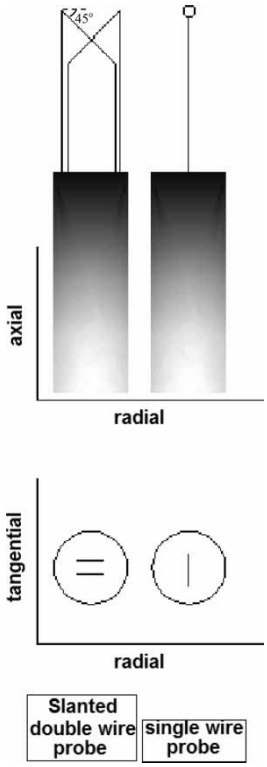


Fig. 4 Description of the hot wire orientation

The hot wire anemometer voltages were first converted to effective wire cooling velocities using King's law, according to which the voltage E is related to the effective cooling velocity U_e by the following relationship

$$E^2 = A + BU_e^c \tag{1}$$

where A is the heat loss through natural convection and conduction along the prongs at zero velocity. The coefficients A, B, and c are determined by calibration of the wire in a wind tunnel [**7**].

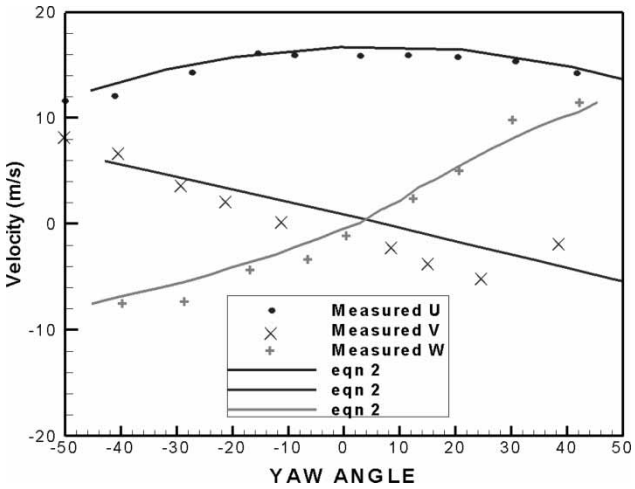


Fig. 5 Directional sensitivity of the wires at zero pitch angle

Directional sensitivity of the wires was undertaken to determine the relationship between the effective wire cooling velocities and mutually perpendicular velocity components. Each of the instantaneous velocity components can be estimated according to Jongensen [**8**] as

$$\begin{aligned} U_{1e}^2 &= k^2 U_n^2 + U_t^2 + h^2 U_b^2 \\ U_{2e}^2 &= h^2 U_n^2 + k^2 U_t^2 + U_b^2 \\ U_{3e}^2 &= U_n^2 + k^2 U_t^2 + h^2 U_b^2 \end{aligned} \tag{2}$$

where U_n, U_t, and U_b are the normal, tangential, and binormal velocity components, respectively, relative to the wire. In this study, the coefficients h and k were determined by changing the wire orientation at fixed wind tunnel speed. The probe was rotated in a range of $\pm 50^\circ$ yaw and 20° pitch angles as shown in Fig. 5. Following the calibration, the measurements were made at 14 axial measurement locations on each passage cross-section for different diffuser locations and flowrates. At each position, readings were performed on each of the 230 shaft revolutions at one-third interval of shaft rotation spanning one impeller passage. The mesh of data points is thus $8 \times 14 \times 57$ in the radial, axial, and tangential directions, respectively. In the case of the vaned diffuser, measurements were repeated at three diffuser vane-to-vane positions (10, 50, and 90 per cent).

2 ANALYSIS OF RESULTS

Mean velocity (equation (3)) and Reynolds stress (equation (4)) components are calculated statistically considering 230 consecutive impeller revolutions at each measurement point. First, equation (1) is used to convert instantaneous voltage readings to the instantaneous effective cooling velocities for each wire. Equation (2) is then used to estimate the instantaneous velocity components

$$\bar{u}_i = \frac{1}{230} \sum_{m=1}^{230} u_i \quad i = r, \theta, z \tag{3}$$

$$u_i'^2 = \frac{1}{230} \sum_{m=1}^{230} (u_i - \bar{u}_i)^2 \quad i = r, \theta, z \tag{4}$$

Similarly the turbulent kinetic energy is calculated statically as

$$q = \frac{1}{230} \sum_{m=1}^{230} \frac{\overline{u_r'^2 + u_\theta'^2 + u_z'^2}}{2U_T} \tag{5}$$

where U_T is the blade velocity at the impeller exit. Reynolds shear stresses ($\overline{u_\theta' u_r'}$, $\overline{u_\theta' u_z'}$, and $\overline{u_r' u_z'}$) are also calculated from the 230 instantaneous tangential, radial, and axial velocities at each measurement point as

$$u_i' u_j' = \frac{1}{230} \sum_{m=1}^{230} (u_i - \bar{u}_i)(u_j - \bar{u}_j) \quad i = r, \theta, \text{ or } z; \quad j = r, \theta, \text{ or } z \tag{6}$$

The error analysis presented by Pinarbasi [**7**] shows that uncertainties in the mean velocity components, the turbulent kinetic energy, and the Reynolds stress components were ± 1 m/s, ± 0.1 and ± 0.05 per cent, respectively. The errors that would occur in measurements were attributed to the assumption of the constant coefficients in equations (1) and (2). More information about the error analysis can be obtained from reference [**7**].

In this paper, the results at two critical stations 1 and 3 are considered. Station 1 is located in the diffuser vaneless space and station 3 is located close to the entry of the vaned region. Before considering the Reynolds stress results, it is necessary to discuss the non-uniformities of the mean flow.

2.1 Mean velocities

Mean velocities are presented as contour diagrams. The contours indicate the magnitude of the radial velocity and the arrows represent the secondary flow formed by the combination of the tangential and axial components. The tangential margins of each diagram for each of the three vane-to-vane positions correspond to consecutive positions where the measurement probe is radially in line with the impeller blade trailing edge.

2.1.1 Station 1

Mean velocity results at station 1 are shown in Fig. 6 for the three inter-vane positions (top 10 per cent, middle 50 per cent, and bottom 90 per cent). The results show that the flowrate adjacent to the vanes is reduced with a corresponding increase in the flowrate midway between the vanes. The peak level of radial velocity midway between the vanes is thus 3 m/s higher than that close to the vanes. Strong cross-flows are observed within the impeller passage wake near the pressure side/shroud surface. This is due to the fact that the enlargement of the wake results in an increased level of flow deficit. The wake is less marked at the 90

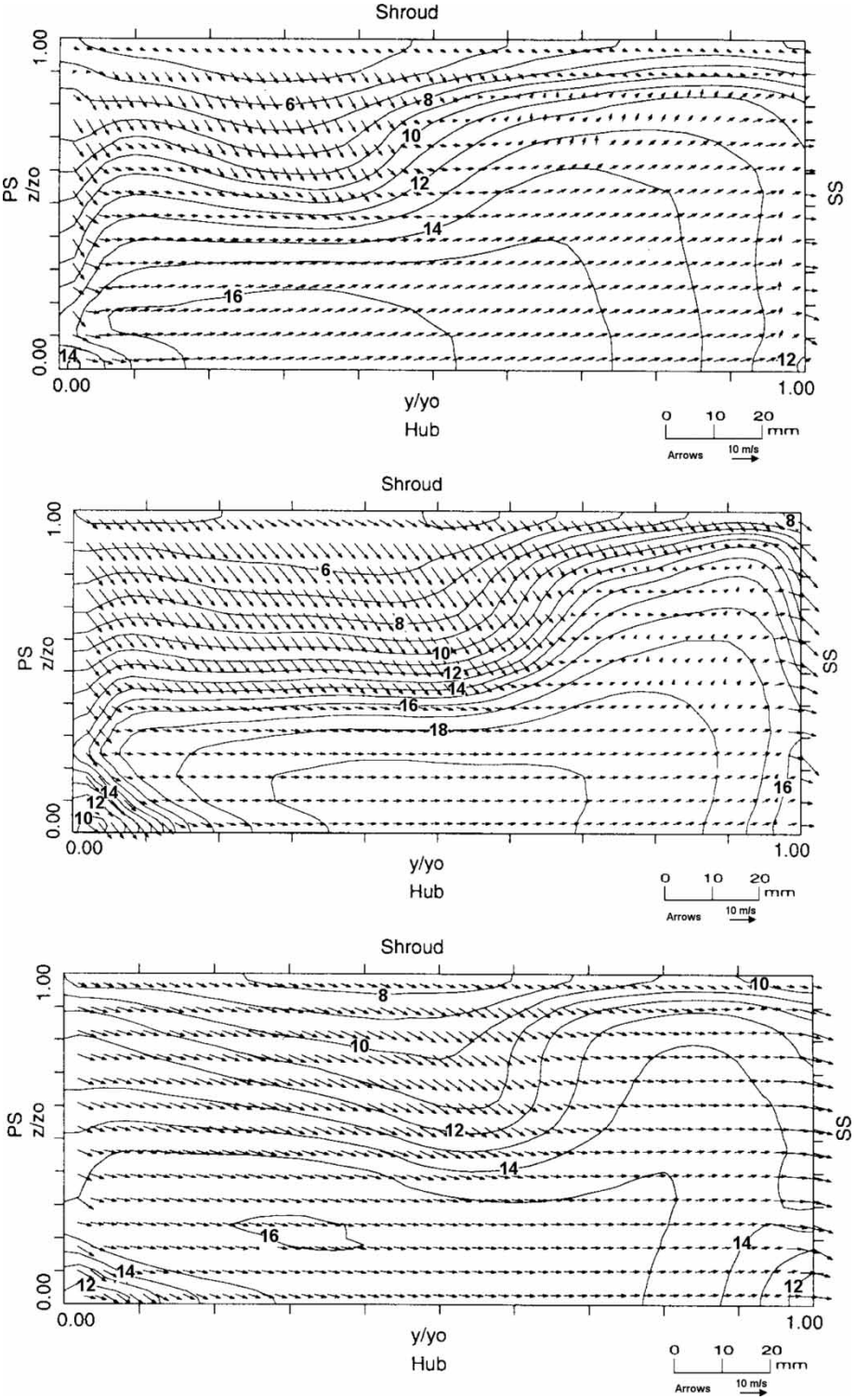


Fig. 6 Mean velocities at station 1 (10, 50, and 90 per cent vane-to-vane position)

per cent vane-to-vane location, which suggests that the pressure in this region may be low.

High shear regions can be identified by the investigation of vorticity components [**7**]. The axial component of vorticity is found to be high in the blade wake regions close to $y/y_0 = 0$ and 1. The axial and tangential components also achieve more modest but significant levels around the edges of the passage wake as depicted by the 10 m/s contours in Fig. 6. The highest magnitude of vorticity is seen at the mid vane-to-vane position. Slightly lower values are observed at the 10 per cent position. At the 90 per cent position, on the other hand, remarkably lower values exist. This is attributed to the existence of low pressure levels at the 90 per cent position and the re-energization of the low momentum and passage wake regions.

2.1.2 Station 3

Station 3 is located just downstream of the vane leading edges. Circumferential velocity variations are generally small as seen in Fig. 7. The blade wake moves in the positive y direction, quickly at the 10 per cent vane-to-vane position and slowly at the 90 per

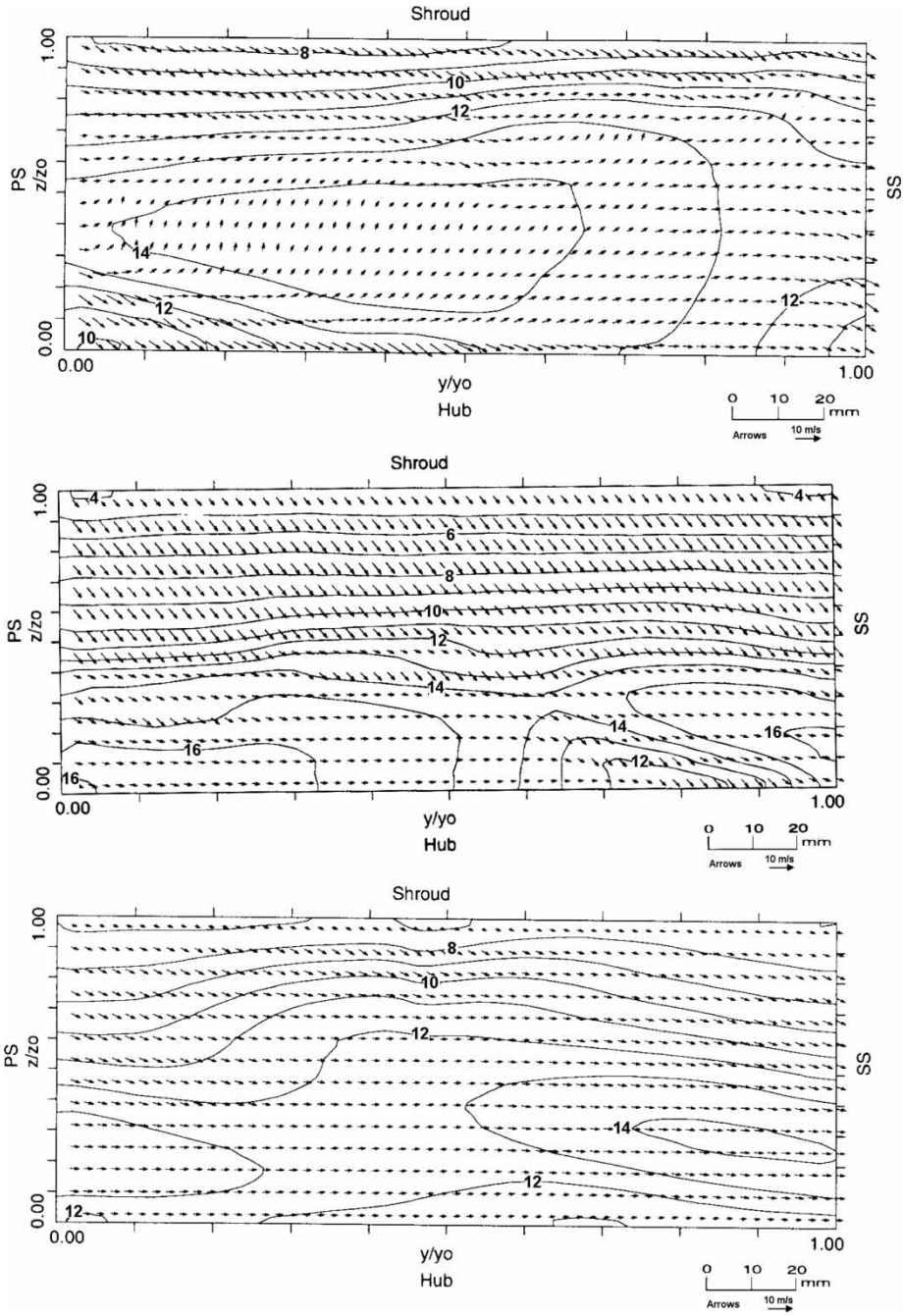


Fig. 7 Mean velocities at station 3 (10, 50, and 90 per cent vane-to-vane position)

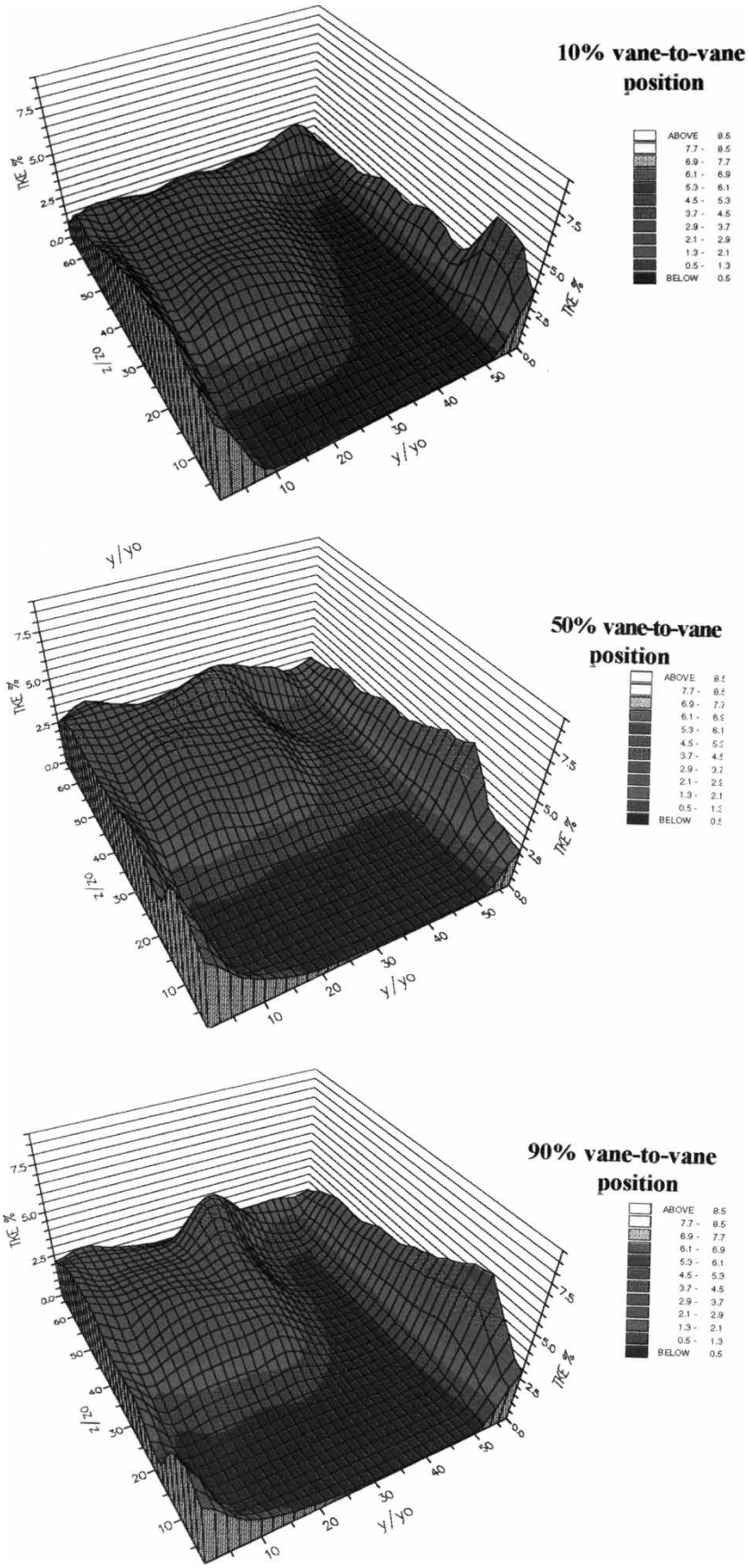


Fig. 8 Turbulent kinetic energy at station 1 (10, 50, and 90 per cent vane-to-vane position)

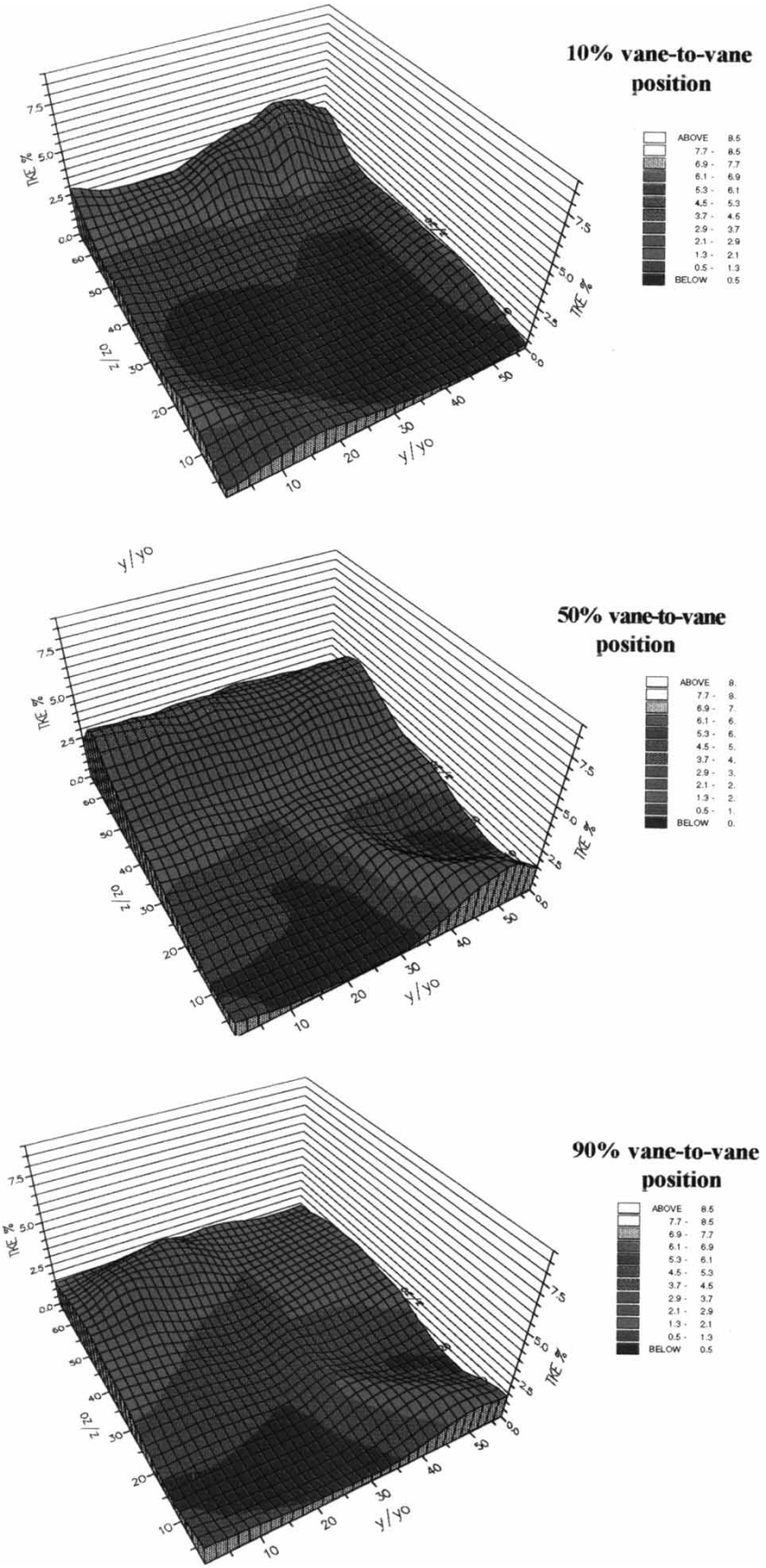


Fig. 9 Turbulent kinetic energy at station 3 (10, 50, and 90 per cent vane-to-vane position)

cent position. The greatest deficit in velocity is found in the blade wake at the mid-vane position, where the strong secondary flow is observed. This is also reported by Krain [**1**] and Inoue and Cumpsty [**2**].

The strength of the shear layers is significantly reduced as compared with station 1, but the maximum and minimum levels remain at the same relative locations.

2.2 Turbulent kinetic energy

2.2.1 Station 1

As shown in Fig. 8, the turbulent kinetic energy distributions indicate a substantial increase in the blade wake. This high level of increase in the blade wake is less than that for a vaneless diffuser downstream of the same impeller [**9**]. This is due to the fact that velocity deficit in the blade wake is reduced in the vaned diffuser as it mixes out more rapidly downstream of the impeller blade. The enhancement of the mixing out is believed to be due to the periodic unsteadiness induced by the diffuser vanes. The levels in the shear layers surrounding the passage wake are similar to those in the blade wake.

2.2.2 Station 3

The position of the blade wake can be seen by the turbulent kinetic energy contours shown in Fig. 9. The

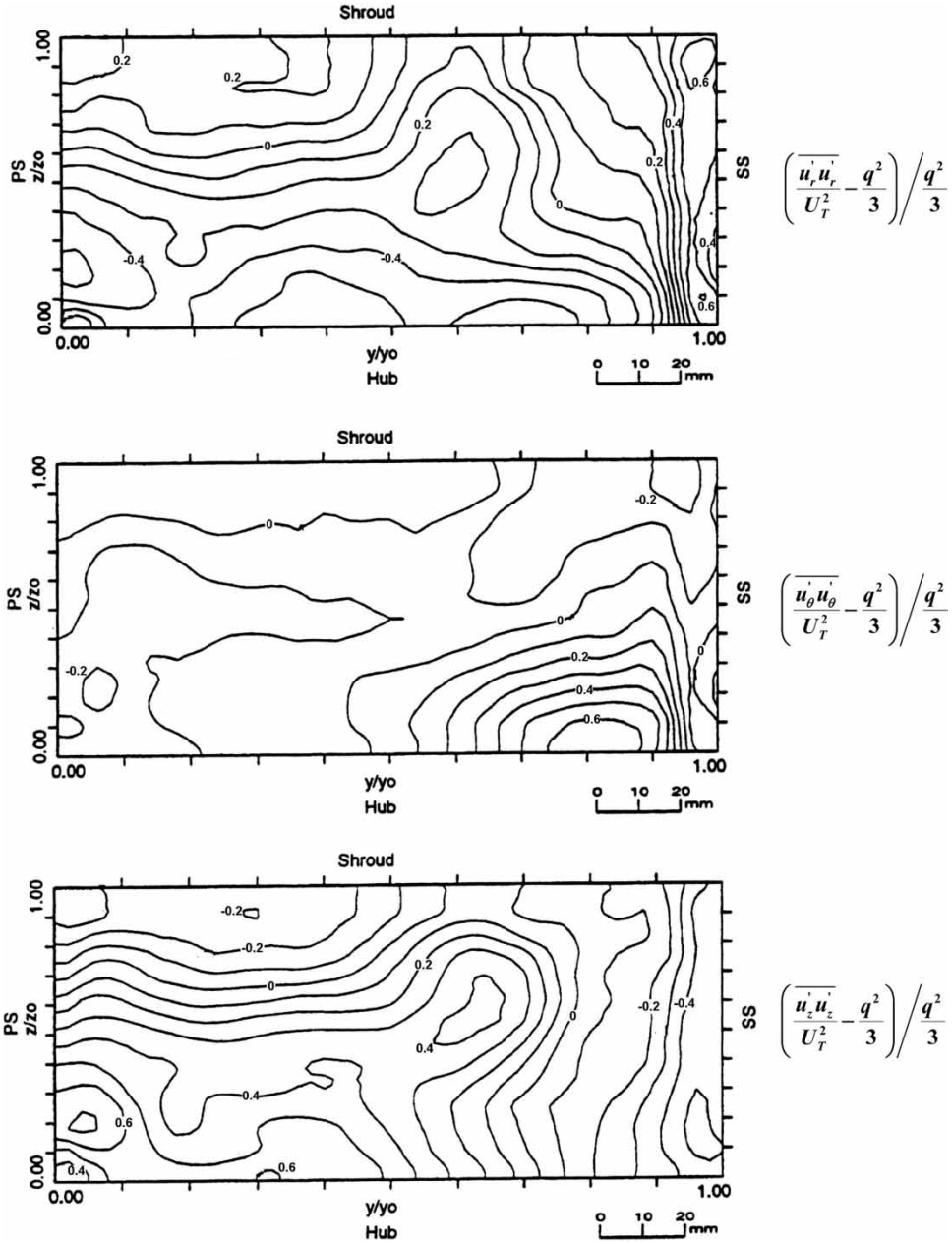


Fig. 10 Non-isotropy factors at station 1

blade wake extends more than one passage width near the hub at the 10 per cent vane position. The distance traversed at the other vane-to-vane positions is shorter. This variation is due to the differences in flow angle, which could also be interpreted as significant changes in the radial velocity component rather than the tangential one.

The level of turbulent kinetic energy within the passage wake at this station is slightly different than that at station 1. However, the distribution of the passage wake is significantly different. Figure 6 shows that the passage wake is diffused almost evenly along the shroud wall. This figure also indicates that the passage wake is

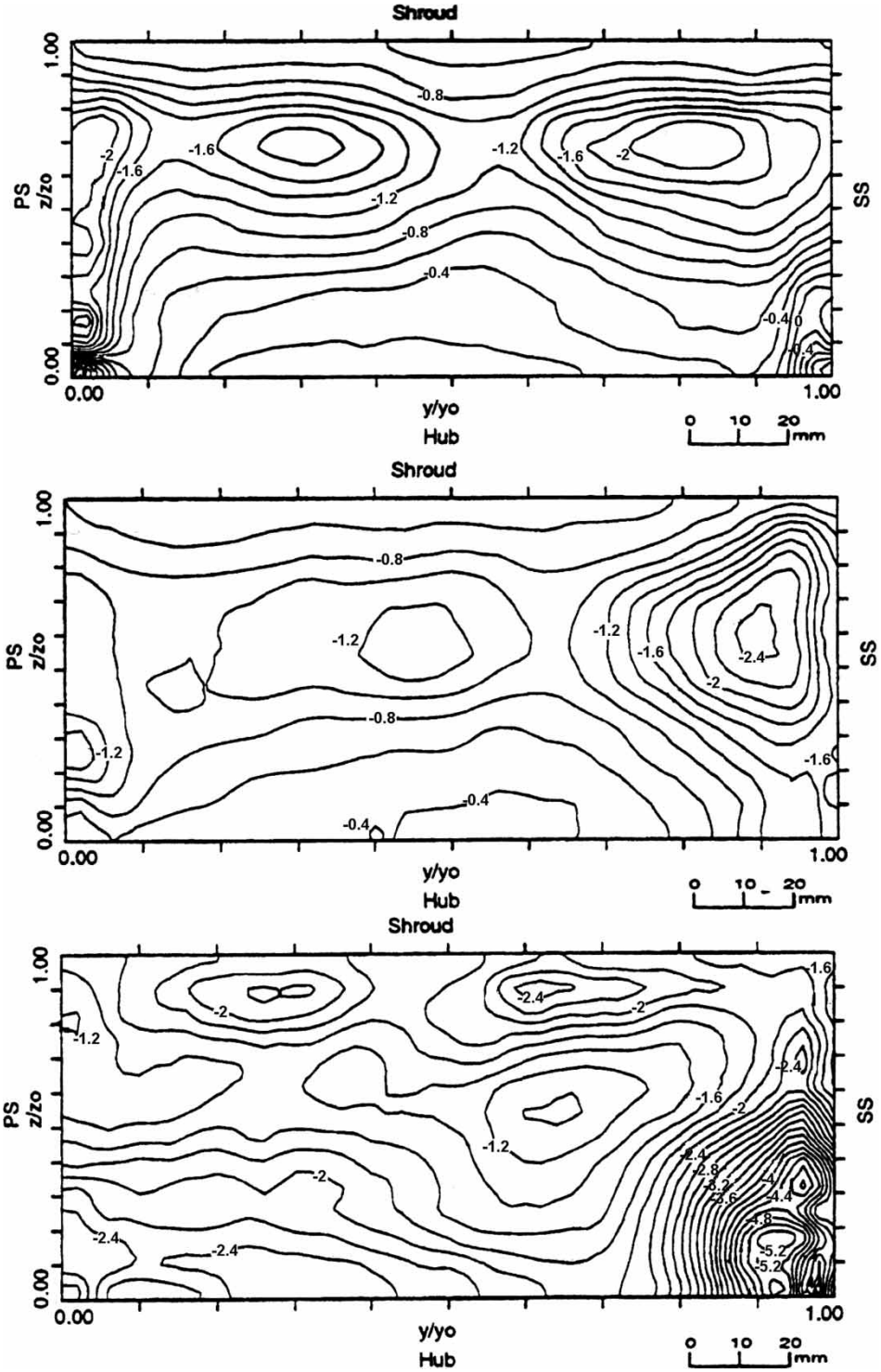


Fig. 11 Reynolds stress component $u_r u_\theta / U_T^2$ (per cent) at station 1 (10, 50, and 90 per cent vane-to-vane)

strong at mid-vane and weak at the 90 per cent position.

2.3 Isotropy

The anisotropy factors shown in equation (7) indicate the degree of isotropy of the turbulence. In equation (7), q is the turbulent kinetic energy normalized by U_T. For isotropic turbulence, all three factors would be equal to zero, whereas for 'one-dimensional turbulence', the factors would be -1, -1, and 2

$$f_r = \frac{\left(\overline{u_r' u_r'}/U_T^2 - 2q^2/3\right)}{2q^2/3}$$

$$f_\theta = \frac{\left(\overline{u_\theta' u_\theta'}/U_T^2 - 2q^2/3\right)}{2q^2/3}, \quad \text{and}$$

$$f_\theta = \frac{\left(\overline{u_z' u_z'}/U_T^2 - 2q^2/3\right)}{2q^2/3} \tag{7}$$

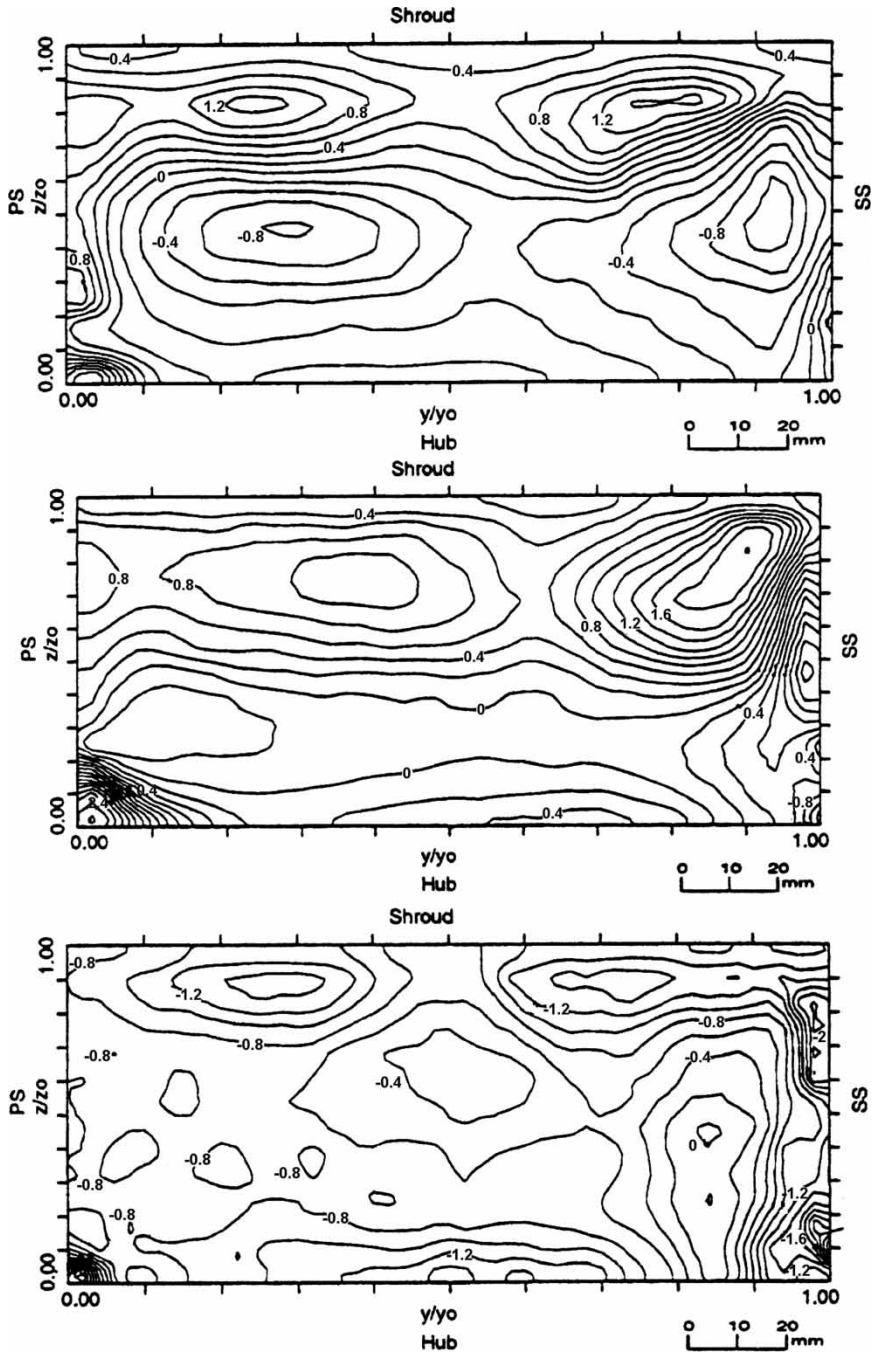


Fig. 12 Reynolds stress component $u_\theta u_z/U_T^2$ (per cent) at station 1 (10, 50, and 90 per cent vane-to-vane)

2.3.1 Station 1

The anisotropy factors suggest that the radial fluctuating component is higher than the tangential and axial components over the suction side half of the passage. Whereas they are lower over the pressure side half of the passage as seen in Fig. 10. This is believed to be an effect of unloading of the impeller blades near the impeller exit. Maximum and minimum values observed at the mid-vane position are seen to

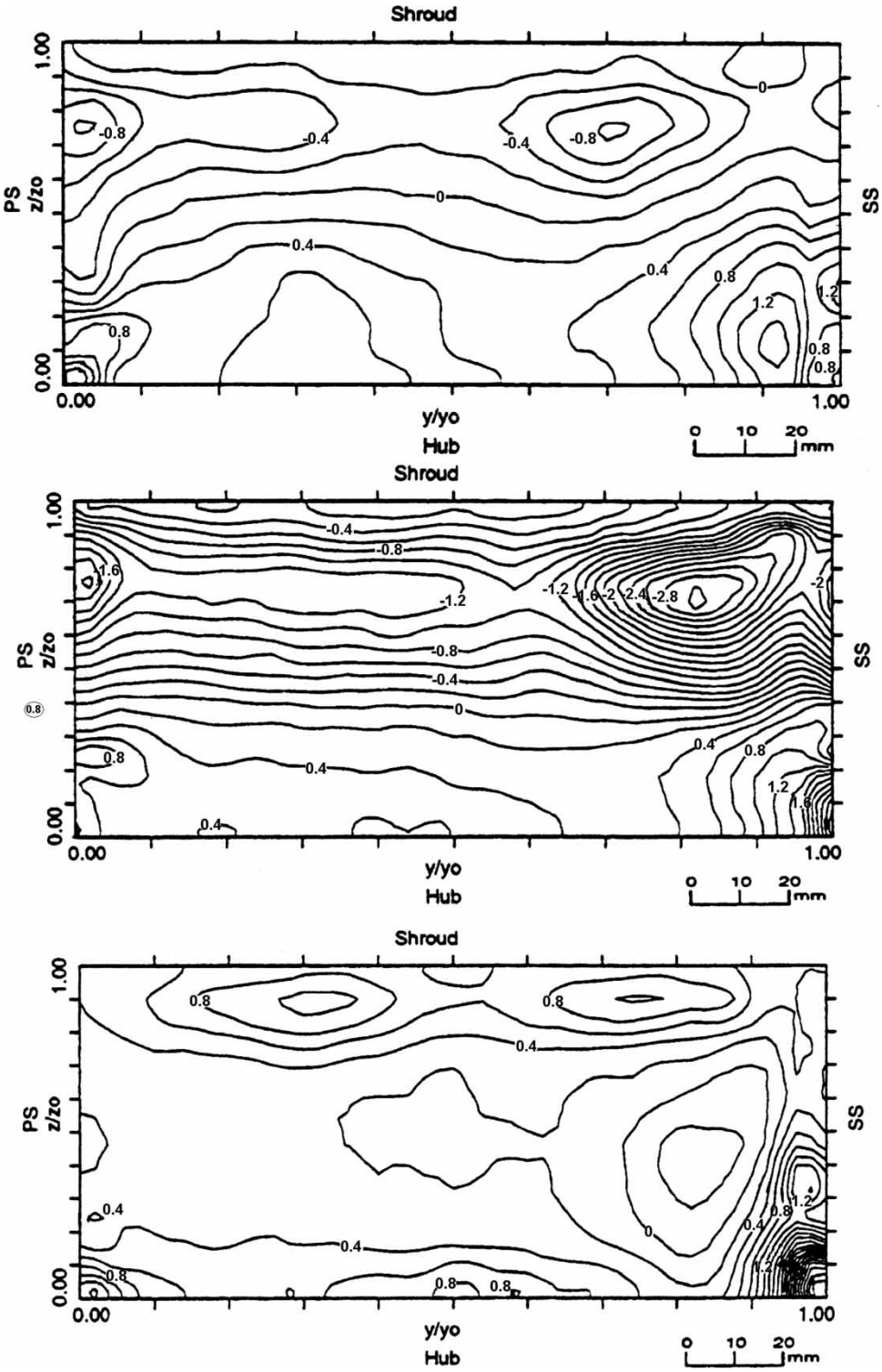


Fig. 13 Reynolds stress component $u_r u_z / U_T^2$ (per cent) at station 1 (10, 50, and 90 per cent vane-to vane)

be 1.5 and −0.75. Values at the 10 and 90 per cent vane positions are generally 45 and 60 per cent low. The factors can be roughly approximated by

$$f_r = -2f_\theta = -2f_z \tag{8}$$

at all vane positions, although there are significant deviations from this relationship within the blade wake.

2.3.2 *Station 3*

At station 3, the flow is highly anisotropic at the mid-vane positions, where f_r varies between 0.4 and 1.4 while f_θ and f_z are generally negative. Extreme values exist in the blade wake region close to the hub. The flow near vane positions is almost isotropic with factors ranging from −0.4 to 0.4 over the majority of the passage. The effect of the diffuser vanes is therefore to breakdown any large-eddy structures (low

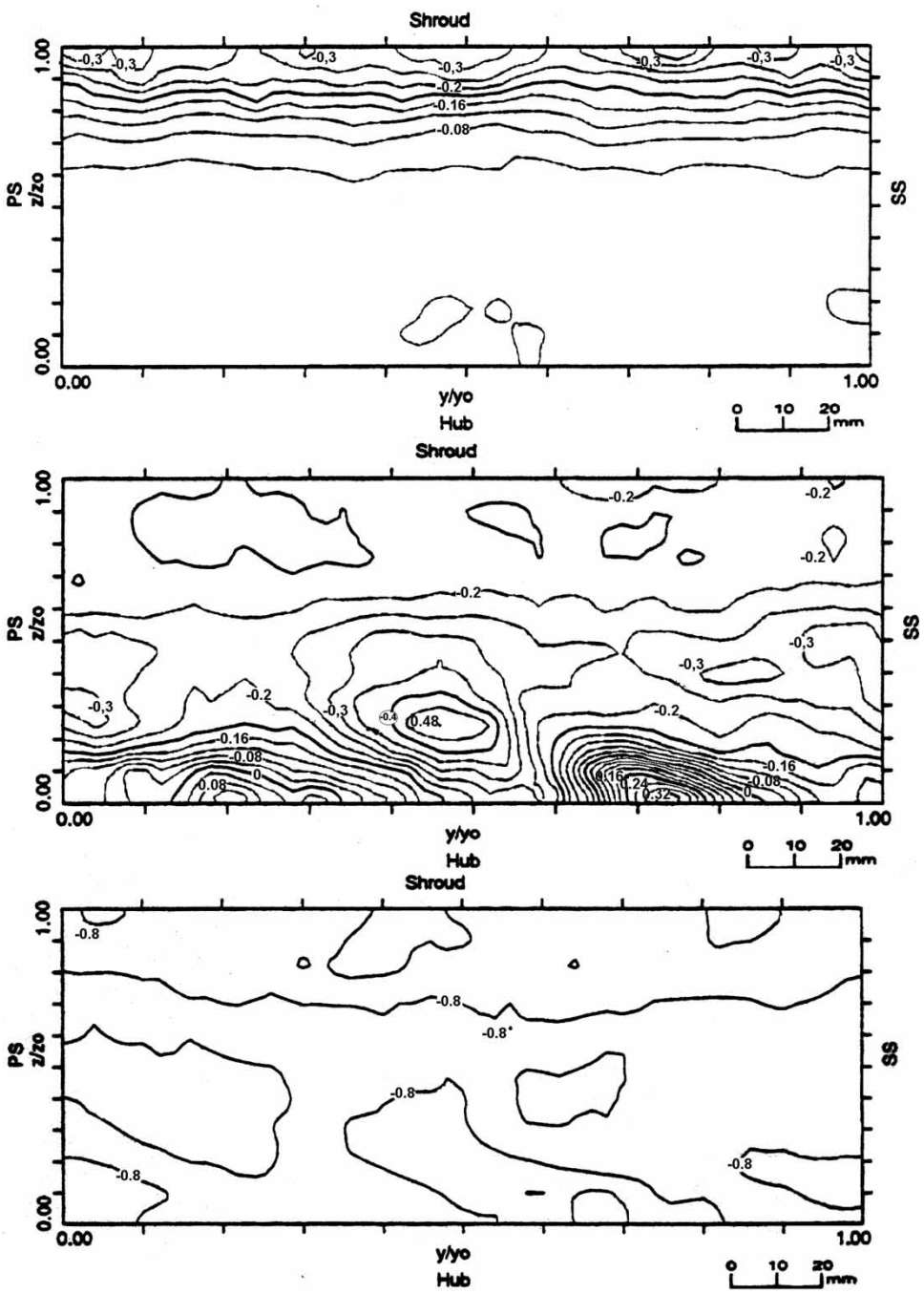


Fig. 14 Reynolds stress component $u_r u_\theta / U_T^2$ (per cent) at station 3 (10, 50, and 90 per cent vane-to vane)

isotropicity) convected from the impeller into smaller structures (high isotropicity).

2.4 Reynolds stresses

2.4.1 Station 1

Reynolds stresses are presented in Figs 11 to 13. Distributions at the mid-vane position are very similar to those observed in the vaneless diffuser. Values are slightly lower than those for the vaneless diffuser. The effect of the vanes is apparent at the 10 and 90 per cent vane-to-vane positions where the Reynolds stresses are generally suppressed. There are increased levels in the suction side/hub corner, within the blade wake and at the 90 per cent vane position. It is clear from these results that the effect of the diffuser vanes extends upstream to the impeller exit.

Similar conclusions can be drawn from the results presented here for a vaned diffuser and from the

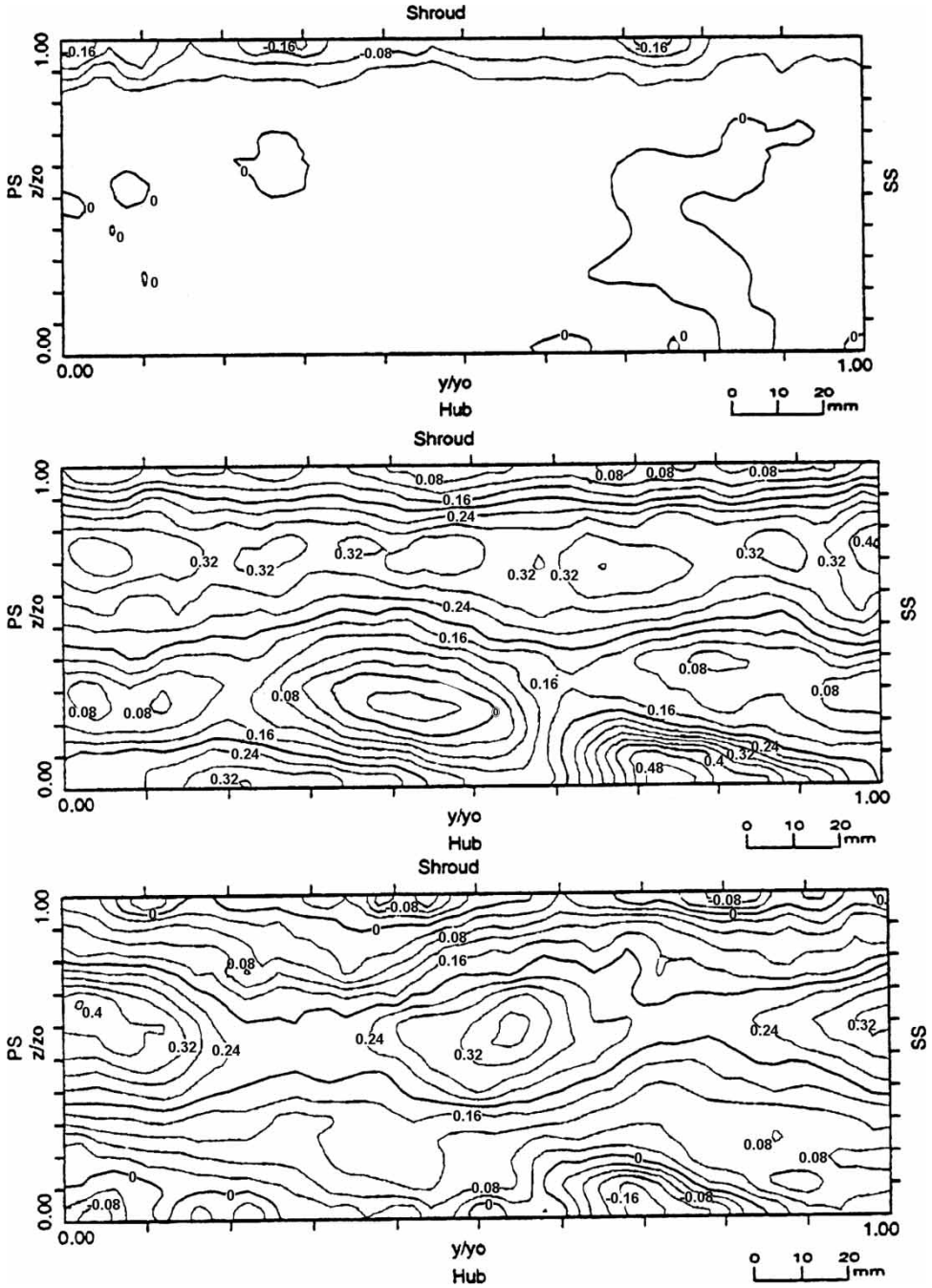


Fig. 15 Reynolds stress component $u_\theta u_z / U_T^2$ (per cent) at station 3 (10, 50, and 90 per cent vane-to vane)

results made by Pinarbasi and Johnson [**10**] for a vaneless diffuser. The Reynolds stresses in the passage wake are generally not higher than that in the entire passage cross-section. This is consistent with slowly mixing out of the passage wake in the diffuser. Another mechanism, to that of turbulence mixing, must therefore be responsible for the high levels of turbulent kinetic energy in the passage wake. It is interesting that if the passage wake changes its position between revolutions, substantial velocity fluctuations exist in the shear layer regions around the passage wake. It is therefore believed that the low frequency meandering in the wake position is responsible for the existence of high levels of turbulence kinetic energy.

High levels of Reynolds stresses are seen to be directly related with the blade wake. They are not located in the centre of the wake, but rather near the suction side around $0.8 < y/y_0 < 0.9$. Bradshaw [**11**] studied the effect of streamline curvature on turbulence within a shear layer. He concluded that where

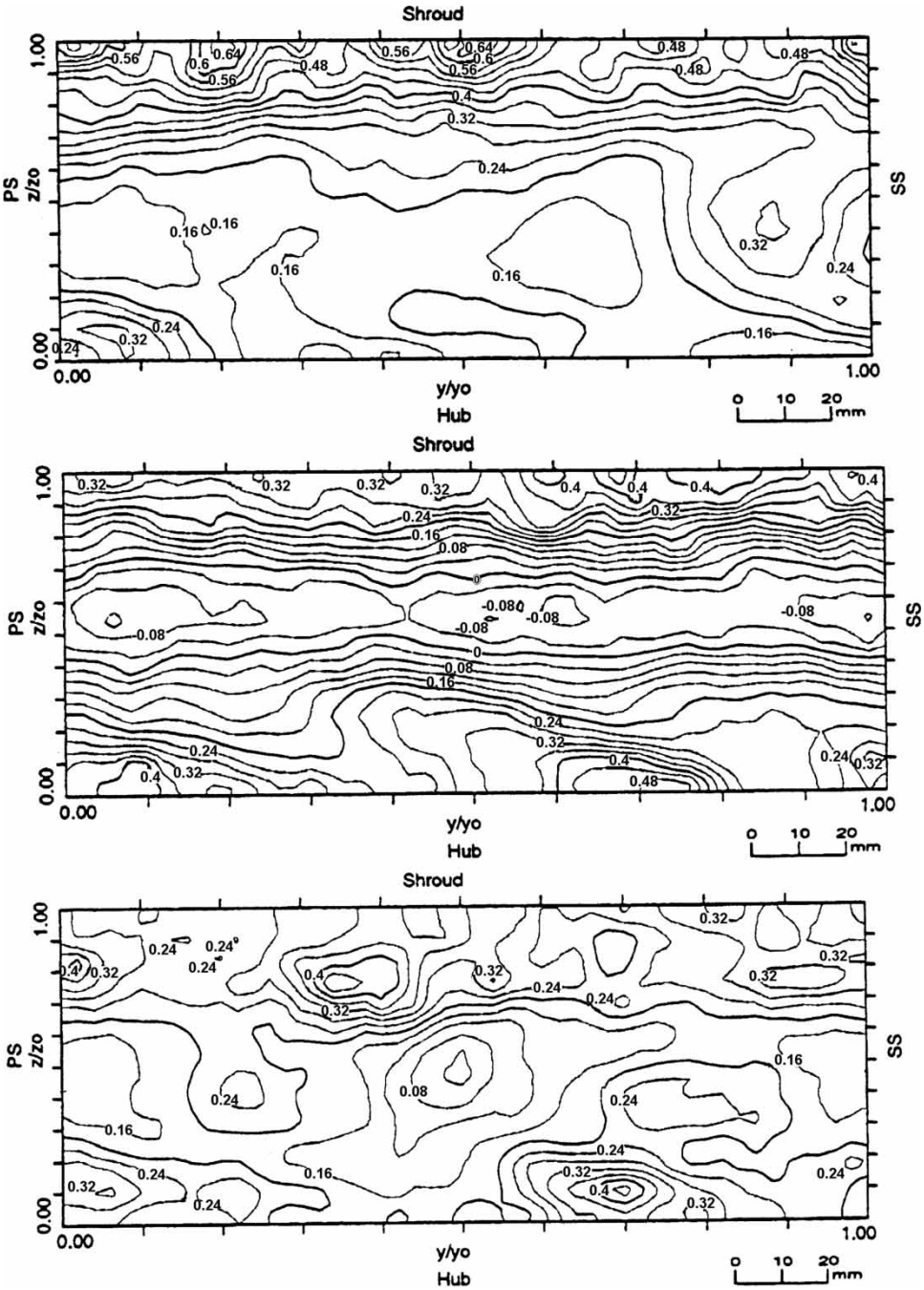


Fig. 16 Reynolds stress component $u_r u_z / U_T^2$ (per cent) at station 3 (10, 50, and 90 per cent vane-to vane)

the velocity increases towards the centre of streamline curvature, the flow is unstable, and this causes high levels of turbulence. When the velocity decreases in this direction, the flow is stabilized and hence turbulence is suppressed. Thus, in the current flow, the streamline curvature results in the destabilization of the shear layer on the suction side and the stabilization of the layer on the pressure side.

2.4.2 Station 3

At station 3 (Figs 14 to 16), the Reynolds stresses are considerably decreased. These are approximately 30 per cent of those at the same station for the vaneless diffuser [**10**].

Variations in the circumferential direction are smaller compared with those in the radial direction. The effect of the vanes is therefore to enhance the early mixing out of the blade wakes in the vaneless space. The level of mixing and Reynolds stresses are low at the inlet of the vaned region. Variations between the vane-to-vane positions are also fairly small, although significant suppression occurs at the 10 per cent location for $u'_r u'_\theta$ and $u'_\theta u'_z$ and enhancement occurs at the 90 per cent location for $u'_r u'_\theta$.

3 CONCLUSIONS

The phase lock loop measurement technique is capable of obtaining accurate detailed measurements in centrifugal compressor diffusers. Measurements show that the flow at the diffuser inlet exhibits similar non-uniformities observed previously at the impeller discharge. It was seen that diffuser vanes significantly influence the flow in the vaneless space. Velocities are increased in the mid-vane position and decreased close to the vanes. Mixing out of the blade wakes is seen to be enhanced.

Mean velocities are slightly decreased and Reynolds stresses are substantially suppressed near the vanes. The passage wake is least marked at the 90 per cent vane-to-vane location due to the low pressure resulting from the vane loading. High levels of turbulent kinetic energy are observed in the wake regions. Reynolds stresses are seen to be lower in the passage wake, which mixes out slowly. Comparisons with results in a vaneless diffuser suggest that the presence of the vanes accelerates this mixing out process.

Streamline curvature is observed to stabilize the shear layers as supported by the variations in Reynolds stresses. The flow is highly anisotropic, particularly at the mid-vane position. Destabilization of the flow is also seen. This multi-scaled characteristic of the flow suggests that the standard one- and two-equation models, most of which are based on the isotropy of turbulence, would not reveal all the features of the flow in a centrifugal compressor with a vaned diffuser. It is well known that these models do not include the effects of Coriolis and centripetal force. It is suggested that the advanced unsteady Reynolds stress models or large eddy simulations are needed for accurate predictions of the mixing out processes and hence the overall losses. Authors would recommend the twisting of the vane leading edge in the axial direction in order that the risk of flow separation is minimized.

REFERENCES

1 **Krain, H.** A study on centrifugal impeller and diffuser flow. *ASME J. Eng. Power*, 1981, **103**, 688–697.
2 **Inoue, M.** and **Cumpsty, N. A.** Experimental study of the centrifugal impeller discharge flow in vaneless diffusers. *J. Eng. Gas Turbines Power*, 1984, **106**, 455–467.
3 **Davis, M. C.** and **Flack, R. D.** Laser velocimetry measurements in a laboratory vaned diffuser. *Expl. Fluids*, 1990, **9**, 33.
4 **Yoshinaga, Y., Gyobu, I., Mishina, H., Koseki, F.,** and **Nishida, H.** Aerodynamic performance of a centrifugal compressor with vaned diffusers. *ASME J. Fluids Eng.*, 1980, **102**, 486–493.
5 **Maksoud, T. M. A.** and **Johnson, M. W.** Stress tensor measurements within the vaneless diffuser of a centrifugal compressor. *Proc. Instn Mech. Engrs, Part C: J. Mechanical Engineering Science*, 1989, **203**(C1), 51–59.
6 **Pinarbasi, A.** and **Johnson, M. W.** Off design flow measurements in a centrifugal compressor vaneless diffuser. *J. Turbomach.*, 1995, **117**(4), 602.
7 **Pinarbasi, A.** *Flow investigation in centrifugal compressor vaneless and vaned diffuser*. PhD Thesis, University of Liverpool, 1995.
8 **Jorgensen, F. E.** Directional sensitivity of wire and fibre film probes. DISA Information no. 11, 1971, pp. 31–37.
9 **Pinarbasi, A.** and **Johnson, M. W.** Detailed flow measurements in a centrifugal compressor vaneless diffuser. *J. Turbomach.*, 1994, **116**(3), 453–461.
10 **Pinarbasi, A.** and **Johnson, M. W.** Detailed stress tensor measurements in a centrifugal compressor vaneless diffuser. *J. Turbomach.*, 1996, **118**(2), 394–399.
11 **Bradshaw, P.** Effects of streamline curvature on turbulent flow. AGARDograph 169, 1973.

APPENDIX

Notation

A, B, c	King's law calibration coefficients
E	hot wire anemometer voltage
f_r, f_θ, f_z	radial, tangential, and axial anisotropy factors
H, K	directional coefficients for hot wire
L	radial distance from impeller outlet

q	non-dimensional turbulent kinetic energy
R_o	impeller outlet radius
u_r, u_θ, u_z	tangential, radial, and axial mean velocity components
u'_r, u'_θ, u'_z	tangential, radial, and axial fluctuating velocity components
U_e	effective cooling velocity
U_T	peripheral blade velocity at the impeller outlet
U_n, U_t, U_b	normal, tangential, and binormal velocity components relative to the wire
y/y_0	circumferential coordinate
z/z_0	axial coordinate